Laser-Induced Autofluorescence of Human Arteries

Michele Sartori, Donald Weilbaecher, Giuseppe L. Valderrama, Shoishi Kubodera, Robert C. Chin, Michael J. Berry, Frank K. Tittel, Roland Sauerbrey, and Philip D. Henry

A new technique for imaging the intimal surface of arteries through optic fibers has been devised. With the aid of an optical multichannel analyzer, we recorded in real time fluorescence spectra during excitation of the arterial surface with an argon ion laser. Spectral parameters were used to detect atherosclerotic plaques and to discriminate normal tissue from lipid rich and calcified atheromas. By digitizing relative intensity values and the ratios of the peak at 550 nm to that at 520 nm into a gray scale, we generated pseudocolor maps of the arterial wall of 10 human aortas. Specific color distributions were congruent with the distribution of calcified tissue visualized by soft x-ray radiography and the distribution of lipid delineated by staining with Sudan IV. Thus, bidimensional maps obtained by laser spectroscopy can be used to identify the presence and composition of atherosclerotic lesions. Fluorescence imaging may prove to be an important application of laser techniques for the diagnosis and treatment of atherosclerosis. (*Circulation Research* **1988;63:1053–1059)**

The feasibility of ablating atherosclerotic plaques with laser light transmitted through fiber optic catheters has been conclusively demonstrated,[1–7] but the risk of perforating the arterial wall with this new angioplastic procedure remains an unresolved problem.[8–10] Two factors contribute to perforation: arterial puncture, due to the sharp tip and stiffness of optical fibers, and extension of the laser injury across the arterial wall.[11,12] The transmural extension of the laser injury is the result of an incomplete control of the ablation process. The recent development of blunt fiber tips obtained by arming the fiber ends with metal caps has reduced the risk of perforation.[13] However, such modified tips act only by thermal mechanisms and do not take advantage of direct and specific effects of laser light on tissue. It appears that for laser ablation to become a safe procedure, a monitoring device is needed that yields instantaneous feedback information about the progress of ablation. The device should distinguish between atherosclerotic and nonatherosclerotic tissue and, if possible, provide an estimate of wall thickness. Although angioscopic visualization of the intimal surface may be useful for detection of ruptured atherosclerotic plaques and thrombi,[14,15] surface imaging may not give the structural information required to make laser ablation safe and predictable.[16]

Recently, we have become interested in using low-energy lasers as a diagnostic tool for the characterization of the superficial and deep anatomy of the arterial wall.[17–19] The aim of the present study was to determine whether autofluorescence of arteries induced by low power laser radiation might yield useful information about transmural arterial anatomy. The results indicate that radiation with an argon ion laser at a power well below its ablation threshold induces a fluorescence that can be used to derive arterial maps delineating calcific and noncalcific atheromatous lesions.

Materials and Methods

Fifty-seven segments of fresh human cadaver aortas and 80 segments of coronary arteries collected from 33 different subjects (aged 1 month to 78 years) were used for this study. For each subject, one segment of the thoracic and abdominal aorta

From the Section of Cardiology and Department of Pathology, Baylor College of Medicine, Houston, Texas (M.S., D.W., P.D.H.), and Rice Quantum Institute and Departments of Electrical Engineering and Chemistry, Rice University, Houston, Texas (G.L.V., S.K., R.C.C., M.J.B., F.K.T., R.S.).

Presented in part at the 59th Scientific Sessions of the American Heart Association, Dallas, Texas, November 17–20, 1986.

Supported by grants 1 RO1 HL-36894 and F32-HL-0730801 from the National Institutes of Health, 86G208 from the Texas Chapter American Heart Association, and C-0002 and C-0812 from the Robert A. Welch Foundation. Computational assistance was provided by the CLINFO project, National Institutes of Health Grant RR-00350.

Address for correspondence: Michele Sartori, MD, Baylor College of Medicine, One Baylor Plaza, Houston, TX 77030.

Received November 18, 1987; accepted June 10, 1988.

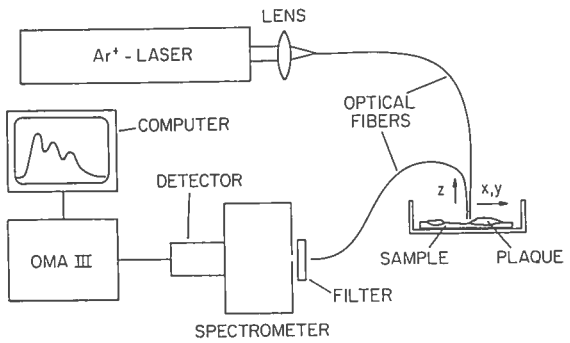

FIGURE 1. *Instrumental setup. An argon laser light is delivered to the tissue sample via an optical fiber. The fluorescence emitted by the tissue is collected by a second fiber and conveyed to a spectrometer equipped with an optical multichannel analyzer (OMA III). The latter is connected to a computer for data storing on disk and processing for image construction.*

and one segment of each of the epicardial coronary arteries were chosen. Segments were selected to obtain an approximately equal number of normal and atherosclerotic specimens. The arteries were opened and pinned intimal side up on a corkboard. Paper rulers were glued to the sides of the arteries as a reference system of the intimal topography. A soft x-ray radiogram of the arterial sample was obtained for identification of calcium deposits within the arterial wall. The corkboard was then mounted on a translational stage.

A prism-tuned continuous wave argon ion laser was used as a source for the fluorescence excitation (Figure 1). The laser radiation was coupled into an optical fiber and delivered to the tissue sample. The excitation intensity at the fiber tip was 400 μW/mm^2. The fluorescence radiation emitted from the tissue surface was guided by a second optical fiber to a spectrometer equipped with an OMA III detector system. The spectral resolution of the optical setup was about 0.5 nm. The fiber for delivery of the laser light and the fiber for the fluorescence collection leading to the spectrometer were mounted parallel and in direct contact to each other in a fixed fiber holder. Both fiber tips were kept perpendicular in close contact to the intimal surface. The core fiber diameter was 600 μm, and all fiber ends were polished. Experiments were initially performed with various argon ion laser excitation wavelengths ranging from long ultraviolet wavelength at 351 nm to visible green light at 514 nm.[17–19] Since 458 nm appeared to discriminate best between normal and atherosclerotic samples, we selected this wavelength for the present series of experiments. A filter with a cutoff wavelength of 470 nm (10% transmission) was employed in front of the spectrometer to suppress the signal at 458 nm due to back-reflected laser light from the tissue. The OMA III was connected to an IBM minicomputer displaying, plotting, and storing on disk the autofluorescence

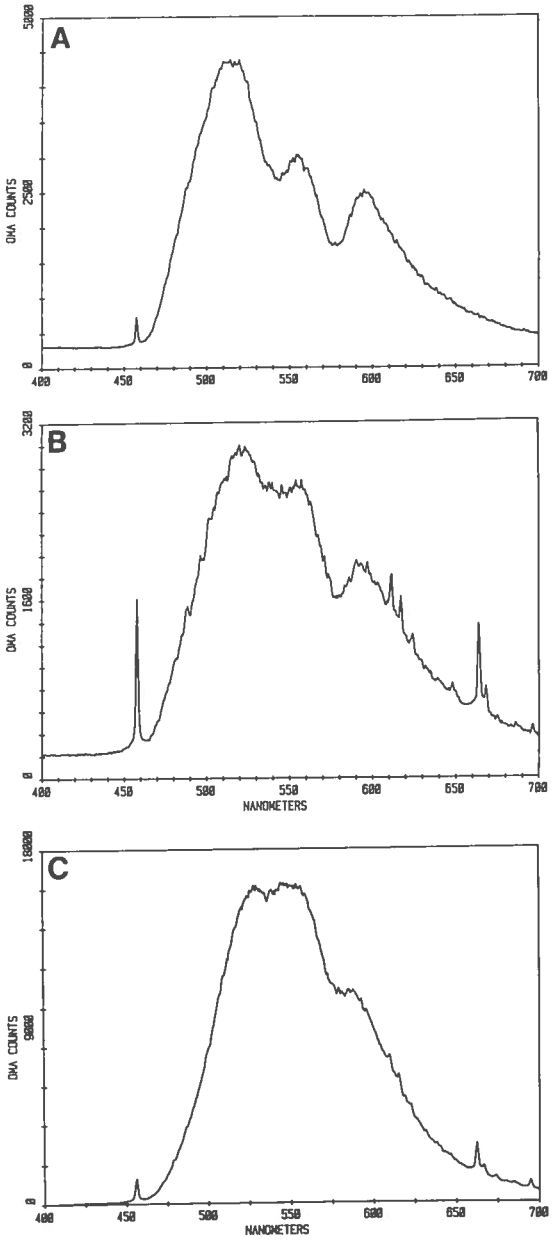

FIGURE 2. *Autofluorescence spectra of human arteries.* A: *Normal left anterior descending coronary artery (LAD). Note the three peaks characteristic of nonatherosclerotic arteries at 520, 550 and 600 nm.* B: *Spectrum of lipid rich plaque of atheromatous LAD. There is almost complete fusion of the peaks at 550 and 520 nanometers. Sharp peaks at 458 nm and other wavelengths are artifacts from the laser excitation source.* C: *Spectrum derived from a calcified segment of LAD. Notice how, in addition to fusion of the first two peaks, the intensity of the fluorescence is remarkably higher than in the normal and lipid rich tissue; 16,000 vs. 4,500, and 3,000, respectively.*

spectra for further processing in an imaging system. The data collection time for a single fluorescence spectrum was 3 seconds.

After collection of each spectrum, the site of the intimal surface probed by the laser beam was marked

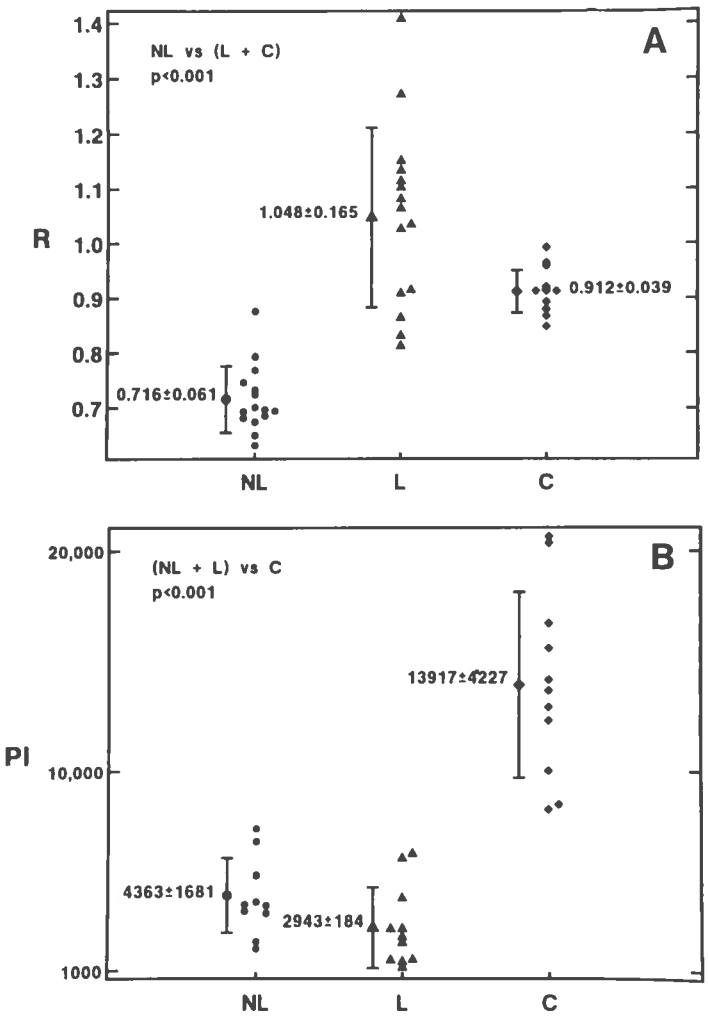

FIGURE 3. A: *Values in arbitrary units of the ratio (R) of the peak intensities at 550 to 520 nm for normal (NL), lipid rich (L), and calcified (C) aortic tissue. A significant difference is found between normal and atherosclerotic tissue.* B: *Peak intensity (PI) values in relative units of the peak at 520 nm for the same three sample groups. The fluorescence intensity of calcified atheromas is approximately four times higher than that emitted by noncalcific plaques or normal tissue.*

with India ink, and the sample was repositioned to excite a new point of the arterial surface. In this way, five to 10 fluorescence spectra were obtained from the same arterial segment. Immediately after fluorescence collection, the samples were dismounted, cut in small tissue segments encompassing single India ink marks, and frozen to liquid nitrogen temperature. Multiple 5 μm thick transverse sections at the level of the India ink mark were then obtained from every tissue block. The sections were alternatively stained with hematoxylin/eosin or Oil Red O. Arterial sites were defined as normal or nonatherosclerotic when no atherosclerotic plaques were evident macroscopically at the site of the fluorescence collection and when light microscopic examination of the sections obtained from the tissue cylinder underlying the site of radiation failed to reveal any of the following changes: 1) intima to media thickness >1.5, 2) accumulation of extracellular or intracellular lipid, 3) accumulation of connective tissue (fibrosis), and 4) accumulation of calcium salts. Atheromas exhibiting positive Oil Red O stain but failing to show bone-dense opacifications by soft x-ray radiography were defined as lipid rich. Areas of tissue appearing as bone-dense structures by x-ray radiography were defined as calcified plaques.

Statistics

All data were expressed as mean±SD. Wilcoxon's rank sum test was used to assess the significance of the difference between group means. A value of $p<0.05$ was considered significant.

Results

Figure 2 illustrates spectra from three arterial tissue types. The fluorescence intensity is plotted versus the wavelength in nanometers. Figure 2A represents an example of a typical fluorescence spectrum obtained from a segment of a normal coronary artery. Three fluorescence peaks are seen at wavelengths of approximately 520, 550, and 600 nm. Sharp peaks are artifacts caused by ion laser plasma tube emissions and by stray light at the excitation wavelength of 458 nm. Figures 2B and 2C illustrate the fluorescence spectra collected from a lipid rich atheroma and a calcified atheroma of the same coronary artery. Compared with Figure 2A, the spectra in Figures 2B and 2C differ by exhibiting increased 550 nm peaks, which fuse with the peaks at 520 nm. Apart from this characteristic spectral change common to both lipid rich and calcified

tissue, the calcified coronary sample is characterized by a pronounced increase in fluorescence intensity. The fluorescence of the calcified sample (Figure 2C) is four times more intense than the fluorescence originating from the normal tissue (Figure 2A) or the lipid rich plaque (Figure 2B). Virtually identical relations between spectral profile and tissue composition were demonstrable for aortic samples, which suggests that the fluorescence-tissue relation depicted in Figure 2 may have general validity for the characterization of arterial tissue.

On the basis of these observations, we first explored the possibility that the change in spectral profile expressed as the ratio of the peaks at 550 nm to those at 520 nm might be useful in differentiating normal from atherosclerotic tissue. Figure 3A is a plot of ratio values for spectra from normal, lipid rich, and calcified samples. Ratio values for atherosclerotic samples were significantly higher than those for normal samples (1.048 ± 0.165 and 0.91 ± 0.04 vs. 0.716 ± 0.061, both $p < 0.001$). Accordingly, it appeared that ratio values in excess of 0.8 were characteristic of atherosclerotic plaques.

Noting a very strong fluorescence intensity at sites of arterial calcification, we then determined whether fluorescence intensities at 520 nm might be useful as a signal for the presence of calcific atheromas. Figure 3B illustrates the intensity values of the peak at 520 nm for areas of normal, lipid rich, and calcified aortic tissue. Peak intensity values for calcified atheromas are significantly higher than normal and lipid rich tissue ($13{,}917 \pm 4{,}227$ vs. $4{,}383 \pm 1{,}661$ and $2{,}943 \pm 1{,}840$, $p < 0.001$). This confirms that calcified tissue, in addition to exhibiting an abnormal spectral profile, is distinguished by a high fluorescence at 520 nm compared with noncalcific tissue.

To determine the relation between atheromas and fluorescence, we removed the atheromatous gruel by microdissection and recorded spectra after dissection. Figures 4A and 4B illustrate the spectral changes before and after atheroma was peeled. Note that the spectrum recorded after complete removal resembles that of a normal artery. Figure 4C shows that ratio values at the site of atherosclerotic lesions were reduced significantly by removal of the plaques. Therefore, it appeared that the presence of atherosclerotic tissue was responsible for the observed changes in fluorescence.

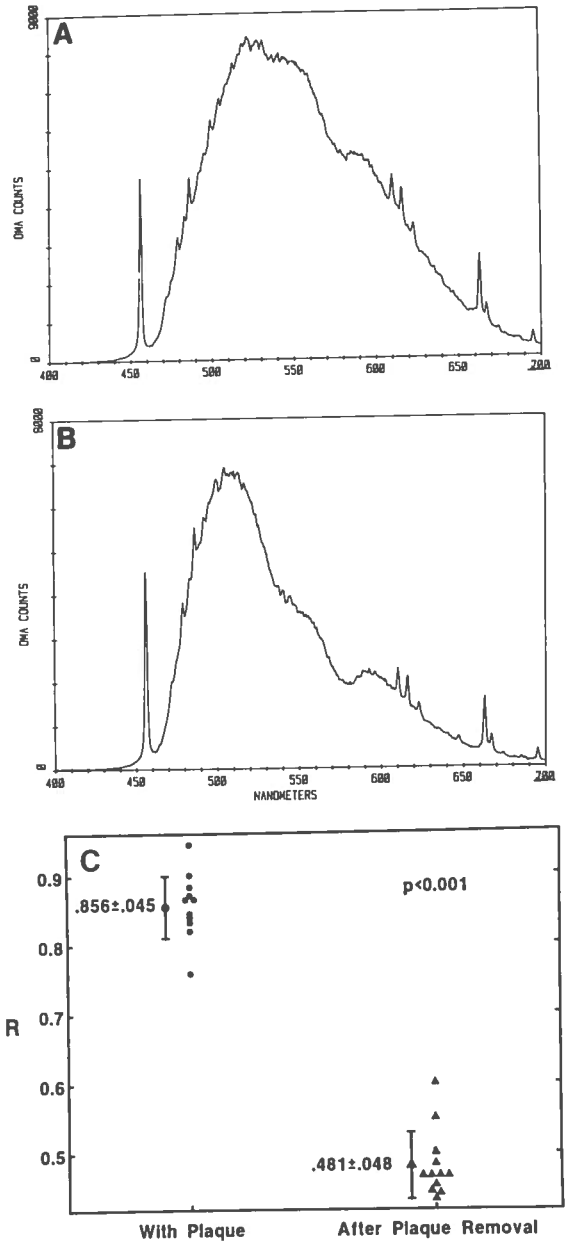

FIGURE 4. *Change in spectral profile of an atherosclerotic aortic sample after removal of the plaque by microdissection.* A: *Before removal;* B: *after removal;* C: *values of ratio (R) (550/520 nm) for 10 sample sites before and after removal.*

Reproducibility of Fluorescence Data

Serial recording of spectra showed that the relative intensities (ratio values) of the fluorescence signals remained unchanged over a 30 minute period. Spectra of arteries kept frozen at liquid nitrogen temperature up to 2 weeks were identical to the spectra of the arteries immediately after harvesting.

Bidimensional Mapping

The parameters derived from the spectral profile (ratio values) and from the peak intensity of the fluorescence spectra (amplitude of the 520 nm peaks) were used to generate bidimensional images of 10 aortic segments exhibiting normal areas alternating with calcified or lipid rich lesions.

A coordinate system producing a square grid (individual square size, 2.5 x 2.5 mm^2) was projected on the arterial surface (Figure 5A). At the site of each intersection of the coordinate lines, an autofluorescence spectrum was recorded and stored on disk. Then the ratio of the 550 to 520 nm peaks and its x,y coordinates were fed into a digital image processor (PSI COM 327). The difference between maximum and minimum ratio values recorded in the

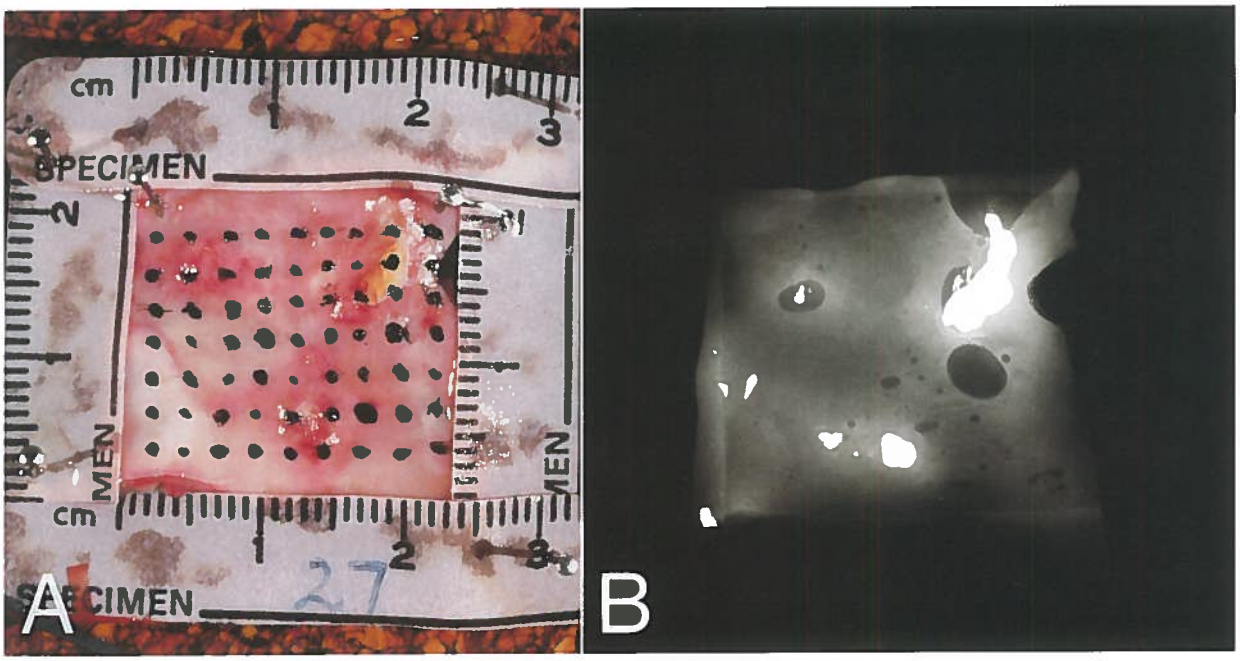

FIGURE 5. *Color photograph and x-ray photograph of a segment of aorta used to generate fluorescence maps.* A: *The aortic segment has been open flat on a corkboard. The black spots at 2.5 mm intervals are India ink marks corresponding to the fluorescence collection sites and are identified in the* x,y *axis by the paper rulers glued to the arterial margins. Lipid rich areas of the intimal surface appear with more intense pink colors because the photograph has been taken after staining the artery with Sudan IV.* B: *Soft x-ray photograph at the same magnification as A. Areas of calcification appear as bone dense structures.*

plane of observation was divided into 128 equal intervals, and a color was assigned to each interval. Red corresponded to the highest, blue to the lowest, and intermediate colors to intermediate ratio values. To generate maps with smooth color transitions a two-dimensional cubic spline interpolation was applied. With the same approach, the peak intensities in relative units at 520 nm were digitized for each *x,y* coordinate to produce maps of fluorescence intensity. The color photograph of an aorta stained with Sudan IV and the radiograph of the same aorta (Figures 5A and 5B) indicate how fluorescence images by the ratio and intensity methods (Figures 6A and 6B) reflected the distribution of calcific and noncalcific plaques. The ratio map (Figure 6A) detects both noncalcific lipid rich lesions (pink or Sudan-positive areas in the photograph) as well as calcific lesions (yellow or Sudan-negative areas in the photograph and bone-dense areas in the x-ray). The intensity map (Figure 6B) localizes a large calcium deposit at the top right corner of the tissue segment. Smaller calcium deposits evident on radiographs are not visualized by the intensity map because the deposits are situated in areas interposed between the sites sampled by laser radiation indicated in the photograph by the black India ink marks.

Since ratio maps distinguished atherosclerotic from nonatherosclerotic tissue and intensity maps calcific from noncalcific tissue, we combined the maps to produce images discriminating the various types of tissue identified by the two fluorescence methods (Figure 6C). The following color assignments were made for the combination maps: 1) black, areas of high ratio and high intensity representing calcific zones; 2) blue, areas of high ratio and normal intensity representing noncalcific lipid rich atheromas; and 3) purple, areas of normal ratio and normal intensity representing nonatherosclerotic (normal) tissue. Note in Figure 6 that black corresponds to the calcific zone detected by x-ray radiography and blue delineates the noncalcific lipid rich (sudanophilic) zones. Nonatherosclerotic zones exhibiting neither radiopaque deposits nor sudanophilia show up in purple.

Discussion

The present study demonstrates that low-power laser-induced fluorescence provides useful information about arterial wall structure. In both aortas and coronary arteries, spectra with high ratios of the peak at 550 nm to that at 520 nm were related to the presence of abnormal accumulations of lipid or calcium. On the other hand, high relative intensity at 520 nm signaled the presence of calcification. By digitization of the ratio and intensity parameters, bidimensional color maps delineating calcific and noncalcific lesions were generated.

Laser spectroscopy for the diagnostic characterization of tissue was first used by Alfano et al.[20] They excited rat organs with an argon ion laser at 488 nm and were able to detect cancerous tissue in liver, prostate, and bladder. Interestingly, the spectra recorded by these authors showed three peaks at

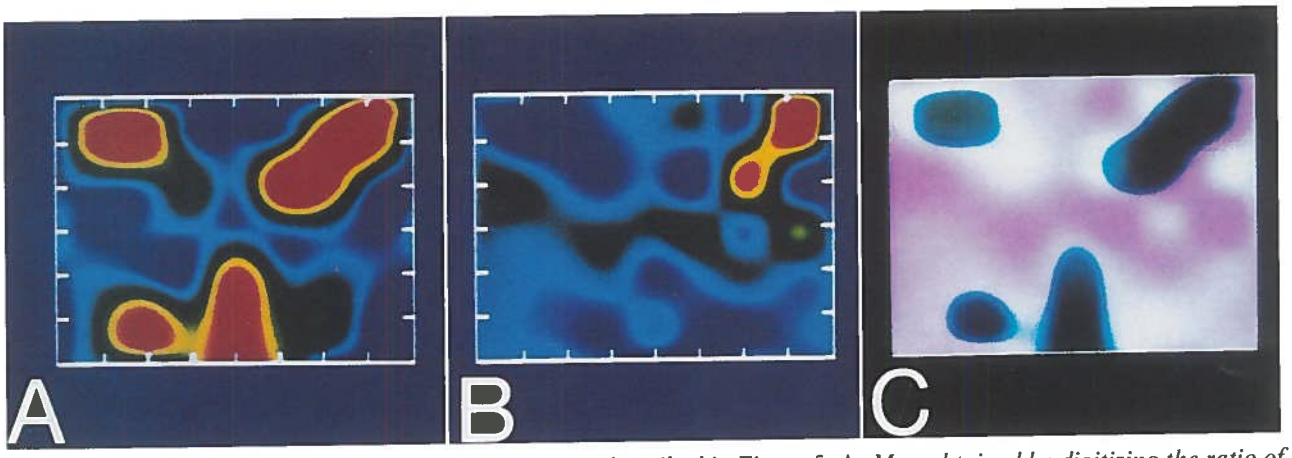

FIGURE 6. *Autofluorescence maps of the human aorta described in Figure 5.* A: *Map obtained by digitizing the ratio of the peak at 550 to 520 nm. All the areas of atherosclerotic tissue (lipid and calcified) appear as yellow and red color. Normal regions are blue.* B: *Map derived by digitizing the intensity of the peak at 520 nm. Only the calcified plaque at the right top corner is visualized.* C: *Map obtained by overlapping A and B. The result is a three color map in which the normal tissue appears in purple, the lipid rich regions in blue, and the calcified region in black.*

approximately 520, 550, and 600 nm, which appear to correspond to the spectral peaks observed in this study. Kittrell et al[21] excited carotid human arteries with an argon laser at 476 nm and observed significant spectral differences between normal and atherosclerotic arteries. However, in their preliminary report, the authors analyzed only the spectral region between 530 and 800 nm such that the peak at 520 nm remained undetected. More recently, two other groups have reported a significant difference in the fluorescence signals derived from normal and abnormal aortas excited by long ultraviolet lasers or visible light.[22,23] It appears that these preliminary reports are in general agreement with the present findings.

The identification of arterial wall fluorophores responsible for the observed atherosclerotic fluorescence changes would require fractionation and extraction of nonatherosclerotic and atherosclerotic tissue and characterization of the fluorescence properties of the extracts. Such studies would be interesting, but might prove complex and difficult. Changes in fluorescence spectra at the site of atherosclerotic lesions might not only reflect changes in the abundance of specific fluorophores, such as flavins,[24] but might be attributed to blood reabsorption phenomena.[25] Surface fluorescence may be the effect of fluorophores that occur in deep arterial wall and emit broad unstructured spectra in the range between 500 nm and 600 nm. Absorptions at 540 nm and 580 nm by blood overlying the deep source of unstructured fluorescence could account for the structured (triple peak) spectra recorded from the intimal surface.

The similarity between the spectra obtained from normal human arteries and normal human lung tissue[26] suggests that fluorophores determining the observed spectral profiles are widely distributed in tissues. Flavins in mitrochondria are well known to exhibit a strong fluorescence in the 500–600 nm wavelength region.

The change in the spectral profile observed with removal of atheromatous material indicates that the presence of atheromas is responsible for the modification of the fluorescence emitted by the arterial wall.

At the present time, the major obstacle to the safe clinical application of lasers has been the risk of perforation. Since the lumen of arteries with advanced atherosclerosis is often eccentric, local arterial wall thickness may vary considerably between neighboring segments and between cross-sectional sectors of the same segments. As a result, minor changes in the direction of laser ablation may either appropriately ablate atheromatous material or lead quickly to perforation. Therefore a fluorescence laser technique able to detect the presence of plaque material may prove very useful. Enhancement of the fluorescence signal could be further achieved by injection of chromophores with selective accumulation in atherosclerotic tissue.[27] The possibility of conveying the excitation light and the emitted fluorescence through optical fibers indicates that fluorescence detection could be performed via a catheter system. With the use of an optical multichannel analyzer, the collection time is reduced to a few seconds, which would permit a characterization of the intimal structure in real time. One could envision a computer-controlled system in which ablation at high power would be under automated control of the low power fluorescence signals.[28,29] The potential significance of our study lies in the demonstration that lasers may be useful for the diagnostic evaluation of atherosclerosis. Experiments in vivo will be required to establish the utility of laser fluorescence as a diagnostic tool.

Acknowledgment

The authors gratefully acknowledge the expert secretarial assistance of Winifred Kearns in the preparation of this manuscript.

References

1. Abela GS, Normann S, Cohen D, Feldman RL, Geiser EA, Conti CR: Effects of carbon dioxide, Nd-YAG, and argon laser radiation on coronary atheromatous plaques. *Am J Cardiol* 1982;50:1199–1205
2. Choy DSJ, Stertzer S, Rotterdam HZ, Sharrock N, Kaminow IP: Transluminal laser catheter angioplasty. *Am J Cardiol* 1982;50:1206–1208
3. Eldar M, Battler A, Neufeld HN, Gaton E, Arieli R, Akselrod S, Levite A, Katzir A: Transluminal carbon dioxide-laser catheter angioplasty for dissolution of atherosclerotic plaques. *J Am Coll Cardiol* 1984;3:135–137
4. Choy DSJ, Stertzer SH, Myler RK, Marco J, Fournial G: Human coronary laser recanalization. *Clin Cardiol* 1984; 7:377–381
5. Abela GS, Normann SJ, Cohen DM, Franzini D, Feldman RL, Crea F, Fenech A, Pepine CJ, Conti CR: Laser recanalization of occluded atherosclerotic arteries in vivo and in vitro. *Circulation* 1985;71:403–411
6. Grundfest WS, Litvack F, Forrester JS, Goldenberg T, Swan HJC, Morgenstern L, Fishbein M, McDermid IS, Rider DM, Pacala TJ, Laudenslager JB: Laser ablation of human atherosclerotic plaque without adjacent tissue injury. *J Am Coll Cardiol* 1985;5:929–933
7. Ginsburg R, Wexler L, Mitchell RS, Profitt D: Percutaneous transluminal laser angioplasty for treatment of peripheral vascular disease. *Radiology* 1985;156:619–624
8. Lee G, Seckinger D, Chan MC, Embi A, Stobbe D, Thomson RV, Sanchez NA Jr, Ikeda RM, Reis RL, Mason DT: Potential complications of coronary laser angioplasty. *Am Heart J* 1984;108:157–159
9. Crea F, Fenech A, Smith W, Conti CR, Abela GS: Laser recanalization of acutely thrombosed coronary arteries in live dogs: Early results. *J Am Coll Cardiol* 1985;6:1052–1056
10. Lee G, Ikeda RM, Chan MC, Lee MH, Rink JL, Reis RL, Theis JH, Low R, Bommer WJ, Kung AH, Hanna ES, Mason DT: Limitations, risks and complications of laser recanalizaton: A cautious approach warranted. *J Am Coll Cardiol* 1985;56:181–185
11. Crea F, Abela GS, Fenech A, Smith W, Pepine CJ, Conti CR: Transluminal laser irradiation of coronary arteries in live dogs: An angiographic and morphologic study of acute effects. *J Am J Cardiol* 1986;57:171–174
12. Isner JM, Donaldson RF, Funai JT, Deckelbaum LI, Pandian NG, Clarke RH, Konstam MA, Salem DN, Bernstein JS: Factors contributing to perforations resulting from laser coronary angioplasty: Observations in an intact human postmortem preparation of intraoperative laser coronary angioplasty. *Circulation* 1985;72:191–199
13. Cumberland DC, Sanborn TA, Taylor DI, Moore D, Welsh CL, Greenfield A, Guben JK, Ryan T: Percutaneous laser thermal angioplasty: Initial clinical results with a laser probe in total peripheral artery occlusions. *Lancet* 1986; 1(8496):1457–1459
14. Grundfest WS, Litvack F, Sherman T, Carroll R, Lee M, Chaux A, Kass R, Matloff J, Berci G, Swan HJC, Morgenstern L, Forrester J: Delineation of peripheral and coronary detail by intraoperative angioscopy. *Ann Surg* 1985; 202:394–400
15. Sherman CT, Litvack F, Grundfest W, Lee M, Hickey A, Chaux A, Kass R, Blanche C, Matloff J, Morgenstern L, Ganz W, Swan HJC, Forrester J: Coronary angioscopy in patients with unstable angina pectoris. *N Engl J Med* 1986; 315:913–919
16. Abela GS, Seeger JM, Barbieri E, Franzini D, Fenech A, Pepine CJ, Conti CR: Laser angioplasty with angioscopic guidance in humans. *J Am Coll Cardiol* 1986;8:184–192
17. Sartori M, Henry P, Roberts R, Chin RC, Berry M: Characterization of intimal structure and thickness in normal and atherosclerotic vessels by argon ion laser induced fluorescence (abstract). *Lasers Surg Med* 1986;6:176
18. Sartori M, Bossaller C, Weilbacher D, Henry PD, Roberts R, Chin RC, Valderrama J, Berry M: Detection of atherosclerotic plaques and characterization of arterial wall structure by laser induced fluorescence (abstract). *Circulation* 1986;74(suppl II):II-27
19. Sartori M, Henry PD, Roberts R, Kubadero S, Sauerbrey R, Valderrama J, Berry M, Tittel FK: Realtime collection of autofluorescence of coronary arteries (abstract). *Lasers Surg Med* 1987;7:131
20. Alfano RR, Tate DB, Corsters J, Tomashefsky P, Longs FW, Alfano MA: Laser induced fluorescence spectroscopy from native cancerous and normal tissue (abstract). *IEEE J Quantum Electronics* 1984;QE20:1507
21. Kittrell C, Willett RL, Santos-Pacheo C, Ratliff NB, Kramer JR, Malk EG, Feld MS: Diagnosis of fibrous arterial atherosclerosis using fluorescence. *Applied Optics* 1985; 24:2280–2281
22. Deckelbaum LI, Lam JK, Cabin HS, Long MB. Discrimination of normal and atherosclerotic aorta by laser induced fluorescence (abstract). *Clin Res* 1986;34:292A
23. Lu DY, Leon MB, Smith PD, Balaban RS: Atherosclerotic plaque identification using surface fluorescence (abstract). *Clin Res* 1986;34:630A
24. Benson RC, Meyer RA, Zaruba ME, McKhann GM: Cellular autofluorescence—Is it due to flavins? *J Histochem Cytochem* 1978;27:44–48
25. Hoshihara Y: Influence of tissue hemoglobin on argon laser induced fluorescence of gastrointestinal mucosa. *Jpn J Gastroenterology* 1985;82:1853
26. Chang-Tung EG, Mountain CF, Chin RC, Berry MJ: Lung cancer detection using laser induced autogenous fluorescence spectroscopy (abstract). *Lasers Surg Med* 1987;7:106
27. Murphy D, Chutorian D, Kosek J, Mok W, Quay S, Huestis W, Mehigan J, Profitt D, Ginsburg R: Selective absorption of ultraviolet laser energy by human atherosclerotic plaque treated with tetracycline. *Am J Cardiol* 1985;55:1293–1297
28. Mehta A, Richards-Kortum RR, Kittrell C, Feld MS; Real time determination of artery wall composition and control of laser ablation using laser induced fluorescence. Conf on Lasers and Electrooptics, April 26–May 1, 1987, Baltimore, Md.
29. Sartori M, Sauerbrey R, Kubodera S, Tittel FK, Roberts R, Henry PD: Autofluorescence maps of atherosclerotic human arteries—A new technique in medical imaging. *IEEE J Quantum Electronics* 1987;23:1794–1797

KEY WORDS • argon ion laser • arterial autofluorescence • atherosclerosis • arterial imaging